D1.2 – Local GNSS Effects

Deliverable ID	**D1.2**
Deliverable Title	**Local GNSS Effects**
Work Package	**WP1**
Dissemination Level	**PUBLIC**
Version	**1.1**
Date	**2018-06-01**
Status	**Final**
Lead Editor	**ISMB**
Main Contributors	**ISMB, ENAC**

Published by the ASTRAIL Consortium

This project has received funding from the European Union's Horizon 2020 research and innovation programme under Grant Agreement No 777561
Call identifier: H2020-S2RJU-2017 | Topic: S2R-OC-IP2-01-2017 – Operational conditions of the signalling and automation systems; signalling system hazard analysis and GNSS SIS characterization along with Formal Method application in railway field

Document History

Version	Date	Author(s)	Description
0.0	2018-01-03	ISMB	First draft with TOC
1.0	2018-02-28	ISMB	First issue
1.1	2018-06-01	ISMB	Added legal notice

Legal Notice

Table of Contents

1 Introduction

This document is the deliverable D1.2 of the ASTRail project; it includes the outcomes of Task 1.3 “GNSS local error modelling” carried out by ISMB with the contribution of ENAC.

1.1 Scope

In the frame of the Shift2Rail (S2R) activities, the Innovation Programme 2 (IP2) – Advanced Traffic Management and Control Systems, described in the S2R MAAP, concerns the enhancement of the traffic management and control system in the rail transport. The introduction of GNSS in safety railway applications is amongst the most concrete expected results of IP2.
In order to enable the use of GNSS, the effects of the main impairments that can affect the GNSS signal in a typical railway scenario have to be assessed: such impairments are Multipath propagation, the Non Line-Of-Sight (NLOS) reception, and the Radio Frequency Interferences (RFI), both intentional and unintentional.
The Multipath propagation and the Non Line-Of-Sight (NLOS) reception, are simulated through a specific channel model: starting from solutions found in literature, some changes have been introduced to obtain a better representation of the railway environment and to allow the use of a Radio Frequency (RF) GNSS signals generator.
RFI will be simulated separately and this document performs a classification of the main sources of interference for the GNSS signal and then selects the most relevant for the railway environment.

1.2 Organization of the document

After the Introduction, this document can be divided in two parts

- Section 2 describes the channel model which simulates the effects of multipath propagation and NLOS reception. The adaptation of a channel model present in the literature is described and then a statistical analysis of the resulting model and of its effects on the receiver performance is presented;
- Section 3 classifies the RFI and select the most relevant ones for the railway environment.

Finally, Section 4 draws some conclusions.

1.3 Related documents

ID	Title	Reference	Version	Date
[RD.1]				
[RD.2]				
[RD.3]				
[RD.4]				
[RD.5]				
[RD.6]				

2 Radio propagation model for GNSS signals in rail scenarios

2.1 Review of existing channel models for land navigation

The most critical factor in GNSS land applications is multipath and non-Line Of Sight (NLOS) propagation. GNSS signals may be reflected by obstacles surrounding the receiver; these reflected signals can interfere with the reception of the signals coming from the satellites introducing an error in the measurements performed by the receiver and, consequently, in the receiver positioning. Moreover, the obstacles may block the LOS signal reducing the availability of the measurements for the Position Velocity and Time (PVT) computation. A realistic evaluation of the amount of such multipath-induced errors can enable a hazard analysis for the railway application, which is a necessary step toward the introduction of the GNSS use.
Some approaches can be found in literature about the assessment of multipath errors in real or realistic environments. For example, [1] collected measurements from GNSS-alone receivers installed on a train. The analysis of the raw measurements requires an accurate estimation of the train position that can be obtained with the fusion of expensive sensors, and a reference receiver with a clear view of the sky. Analogously, [2] used a couple of cameras installed on a train to record the images of the environment along the track. The resulting videos enable to set a pair of elevation masks as a function of the vehicle position and the azimuth of the satellite: these masks enable to predict possible blockages of the LOS [2] and the presence of reflected rays [3].
Works [1], [2] and [3] based the analysis on real environments; alternatively, an artificial environment that mimics the real one could be used. The use of a real environment gives punctual information about a specific scenario, but it depends on the reliability of some reference information which also could be affected by errors. On the contrary, the artificial environment does not require long on-the-field recordings and the reference (ground truth) is intrinsically known. In [4] a Land Mobile Satellite Channel Model (LMSCM) is described, which includes the characteristics of real environments in an artificial simulation: given the statistical characteristics of the major types of obstacles (house fronts, trees, poles) obtained after extensive measurements campaigns in real scenarios, and given the elevation and azimuth of a satellite, plus the velocity and the attitude of the vehicle, this model randomly generates obstacles and traces the reflected rays and the LOS blockages. The representation of signal reflections characterized with non-zero delays, amplitude and phase variations makes the LMSCM a ‘wideband’ model. The model was standardized by the ITU for Earth-space land mobile telecommunication systems in the L band [5].
For example in the two independent works [6] and [7], authors use the LMSCM to simulate the effects of multipath on the tracking of one satellite and assess the multipath-induced errors and the effectiveness of some multipath mitigation techniques.
The major limitation of the LMSCM as defined in [4] and [5] is the fact that possible changes of the environment that may occur along the track are not taken into account. For instance, if an ‘urban’ environment is set at the beginning of the simulation, it is maintained till the end. Furthermore, one instance of the model addresses just one satellite at a time: the simulation of the channel coefficients for a constellation of visible satellites requires separate, independent simulations.
On the other hand, the land mobile satellite (LMS) channel defined in [9] manages the transitions among different types of environment like transitions among different states of a Finite State Machine (FSM), governed by a Markov chain. However, it represents a ‘narrowband’ channel only, i.e., it does not explicitly model the presence of multiple delayed rays with respect to the LOS.

The channel model presented in this document adapts the FSM in [9] for representing the propagation in each environment (scenario) using the wideband LMSCM of [4]. The represented scenarios are ‘urban’, ‘suburban’, and ‘open-sky’. In the channel model, each scenario is implemented as a state managed by a Markov chain whose transition probabilities are based on the speed of the train. Furthermore, all the visible satellites are managed at a time, allowing the coherent simulation of the propagation effects of a set of satellites that are simultaneously present in the visibility mask of a receiver.
This approach enables the use of the channel model as input to a Radio Frequency (RF) GNSS signals generator: in this way it is possible to assess the performance of commercial receivers when exposed to environmental scenarios corrupted by multipath. The usage of a hardware generator allows real-time signal generation, orders or magnitude faster than a MATLAB-based signal generation, and a direct interface with commercial GNSS receivers to test multipath resilience.

2.2 Satellite-rail radio propagation channel model for GNSS

Starting from the LMSCM in [4][5] and the state transition approach in [9], this section describes the features of a channel model suitable to represent the propagation of GNSS signals in a railway environment. The whole design of the model (LOS and reflected rays' coefficients) is performed at Base Band (BB) with MATLAB, then it is adapted to represent Radio Frequency (RF) effects for its inclusion into a hardware signal generator.

The major features of the developed channel model can be summarized in the following elements:

1. **Identification of the environmental scenarios** encountered by the train during its movement. Three different scenarios have been identified, according to the number and geometry of obstacles involved; these scenarios are implemented as **three states** in the channel model:

    a. an ***open sky*** scenario, characterized by few obstacles (poles, trees and a limited number of buildings); in the case of railways application, the poles represent the power supply arches and are located at a deterministic distance from each other;
    b. a ***suburban*** scenario, characterized by an increased presence of obstacles (e.g. poles, trees and moderate number of buildings);
    c. an ***urban*** scenario, characterized by a remarkable number of obstacles (high number of buildings).

2. **Transition among the scenarios**. In the channel model implementation, it is handled by a Markov chain approach [9]: at any scenario there is a certain probability to stay in the same scenario or to move to a different one.

3. **Correlation with the train speed**. The speed of the train has significant impact on the local propagation effects and therefore on the most likely scenario. Indeed, some associations between the speed of the train and the propagation scenario are unlikely (e.g. a train moving slowly is an uncommon event in an open sky scenario and, conversely, a train moving fast is a rare event in an urban environment). Therefore, the probability of being in a certain scenario in a given instant is determined by the speed of the train in that instant. Furthermore, the speed also determines the frequency at which the scenario may change: the higher the speed of the train is, the more frequently a state transition could take place. We define as a "***segment***" the distance between two consecutive choices (draws) of the scenario.

4. **Local channel effects**. During each segment, the model produces the channel parameters, which comprise the amplitude, phase and delay associated to the reflected rays and the Line-of-Sight (LOS). In order to represent the multipath component with a sufficient resolution, each segment is further divided into ***time bins*** that are constrained to respect the following condition:

$$t_{bin} \leq \frac{\lambda}{8 \cdot v}$$

where v is the velocity of the train and λ is the wavelength of the L1 satellite signal. For example, the following table reports t_{bin} for some sample values of the train velocity.

v (km/h)	t_{bin} (ms)
50	1.7
70	1.2
120	0.7

Notice that the original LMSCM selects the features of the obstacles and their statistics at the beginning of the simulation, then they remain fixed. In the proposed implementation, these features may change at each new segment.

5. **Antenna pattern and Tunnels**. From the LMSCM it is possible to extract the position of the receiver and those of the reflectors. From those, we can calculate the Angle of Arrival (AoA) of the reflected signals to the receiver's antenna. The information of AoA may be exploited to simulate the effect of a non-omnidirectional antenna on the received signal, for example to mitigate the multipath effects. Furthermore, in order to have a more realistic description of railways scenarios, long duration outages (e.g. tunnels) can be generated, described on the basis of the probability of get a tunnel on the simulated track, inter-tunnel distance and the tunnel length. When a tunnel is extracted at the state drawn, then no signals are generated for the whole duration of the outage.

2.2.1 Reference tracks

The starting point for the simulation of the channel model is the definition of the train trajectory.

A *trajectory* is described by three elements, each one represented by a time series: the *time*, the *position* and the *velocity* of the train.

The velocity of the train along the trajectory determines the statistics of the transitions among states, as well as the segment and time bin durations, as explained above. Two different kinds of trajectories can be considered:

- *artificial trajectories*, generated ad hoc in order to have full control of all the simulation conditions;
- *realistic trajectories*, which mimic the real movement of a train along a real portion of railway and can be extracted from the log of a positioning system mounted on a train.

Each reference trajectory, once associated to the simulation of the *propagation channel*, gives rise to a ***reference track*** (see Figure 1).

In view of the assessment of the propagation effects modeled by the simulated channel, a short list of reference tracks has been identified and reported in Table 1. [other tracks may be added]

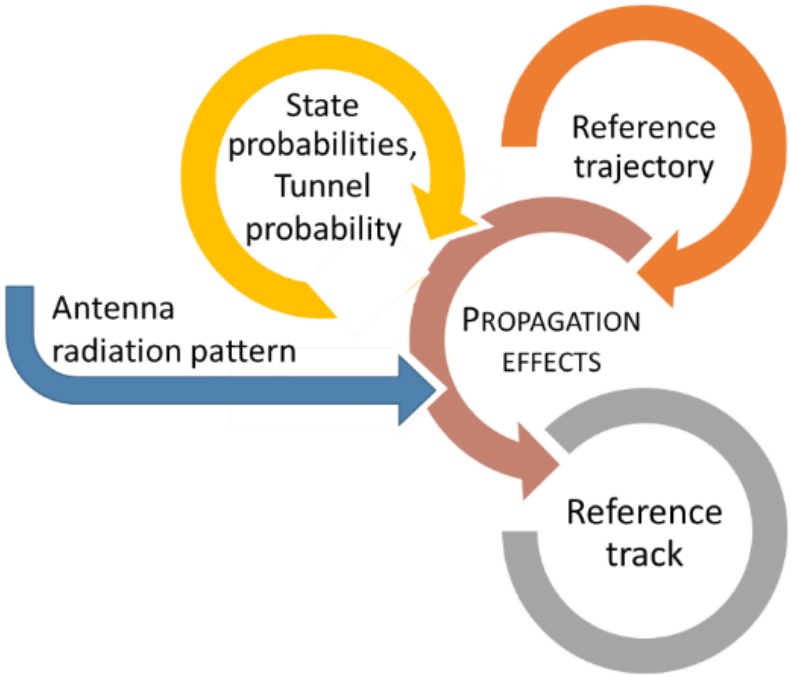

Figure 1. Logic of definition of a reference track

Track ID	Kind of trajectory	Trajectory description	Duration	Distance over ground	Tunnel	Antenna radiation pattern	Goal
Tr01	Artificial	Straight trajectory, medium latitude (45.06°). Constant low speed (50 km/h)	3’	2.5 km	None	Omni directional	To represent the condition of an *urban scenario*
Tr02	Artificial	Straight trajectory, medium latitude (45.06°). Constant medium speed (90 km/h)	3’	4.5 km	None	Omni directional	To represent the condition of a *suburban scenario*
Tr03	Artificial	Straight trajectory, medium latitude (45.06°). Constant high speed (130 km/h)	3’	6.5 km	None	Omni directional	To represent the condition of an *open-sky scenario*
…							

Table 1. List of reference tracks

This project has received funding from the European Union’s Horizon 2020 research and innovation programme under Grant Agreement No 777561
Call identifier: H2020-S2RJU-2017 | Topic: S2R-OC-IP2-01-2017 – Operational conditions of the signalling and automation systems; signalling system hazard analysis and GNSS SIS characterization along with Formal Method application in railway field

2.2.2 Porting on the HW generator: necessary simplifications

The designed channel model has been ported into an RF GNSS hardware generator. The limited number of HW channels available in the generator has required the simplification to a much **reduced number of rays beyond the LOS**, to support a sufficient number of satellites that does not degrade the PVT solution.
The first simplification proposed and assessed is the **two-ray model**, represented by the LOS and one reflected signal. To assess the suitability of such simplification, some metrics have been evaluated: *power profile dispersion, coherence bandwidth* and *coherence time*.

The **HW model** selects the **combination of ray parameters** whose resulting parameters are more statistically similar, according to those metrics, to the case of the multi rays model.

2.2.2.1 *Statistical characterization of the HW model on the reference tracks*

In order to analyze the effects of the simplifications required to implement the HW model, different statistical parameters are analyzed. A summary of the analysis executed on the two-ray model is reported in the following paragraphs.
It must be noticed that, in the following simulations, the fading process of the LOS ray is neglected, to isolate and analyse the effect of the multipath.

2.2.2.1.1 *Time dispersion parameters*

These parameters include the *mean excess delay, RMS delay spread* and *excess delay spread*. The **mean excess delay** is the first moment of the power delay profile and is defined as:

$$\tau = \frac{\sum_k \alpha_k^2 \cdot \tau_k}{\sum_k \alpha_k} = \frac{\sum_k P(\tau_k) \cdot \tau_k}{\sum_k P(\tau_k)}$$

where α_k is the amplitude of the *k*th-component that arrives at the receiver and $P(\tau_k)$ is the power of the *k*th-component.
The ***RMS delay spread*** is the square root of the second moment of the power delay profile and is stated as:

$$\sigma_\tau = \sqrt{\overline{\tau}^2 - (\overline{\tau})^2}$$

where $\overline{\tau}^2 = \frac{\sum_k \alpha_k^2 \cdot \tau_k^2}{\sum_k \alpha_k^2}$. Typical values of delay spread are in the range of nanoseconds. For example, considering the trajectory Tr01 defined in Table 1, the power delay profile is shown in Figure 2.

This project has received funding from the European Union's Horizon 2020 research and innovation programme under Grant Agreement No 777561
Call identifier: H2020-S2RJU-2017 | Topic: S2R-OC-IP2-01-2017 – Operational conditions of the signalling and automation systems; signalling system hazard analysis and GNSS SIS characterization along with Formal Method application in railway field

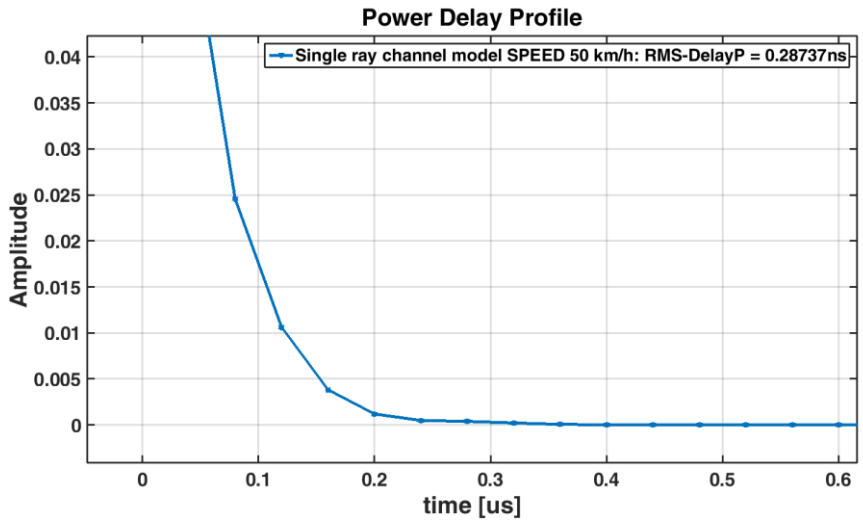

Figure 2. Tr01: RMS delay spread for a single ray channel model.

2.2.2.1.2 *Frequency dispersion parameters*

To characterize the channel in the frequency domain, we have the following parameters.

a) Coherence bandwidth:

It is a statistical measure of the range of frequencies over which the channel can be considered to pass all the frequency components with almost equal gain and linear phase. When this condition is satisfied then we say the channel to be *flat*. The coherence bandwidth describes the time dispersive nature of the channel in the local area.
Figure 3 shows an example of frequency response to evaluate the coherence bandwidth of the channel model, measured on the reference track Tr01.

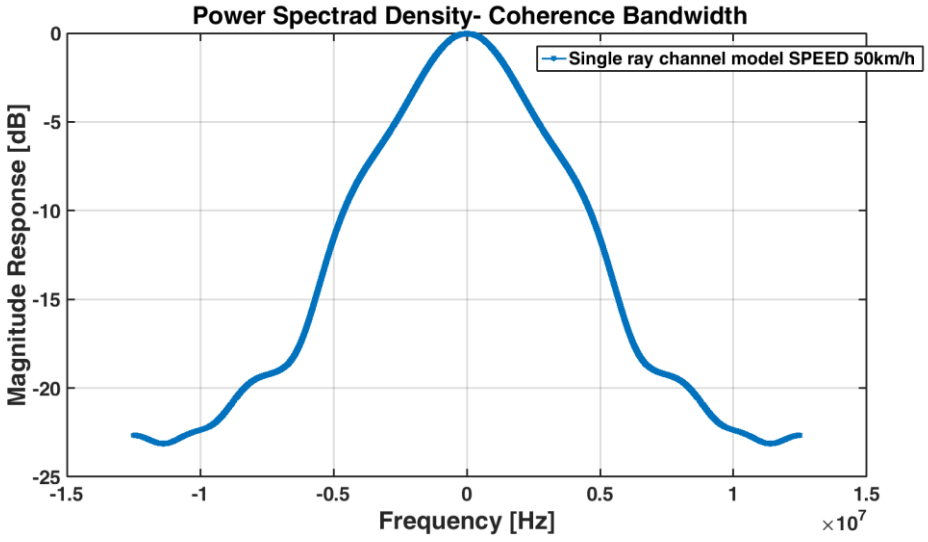

Figure 3. Tr01: Coherence Bandwidth for a single ray channel model.

b) Coherence time:

This is a statistical measure of the time duration over which the channel impulse response is almost invariant. When channel behaves like this, it is said to be slow faded. Typical values of duration are tens of milliseconds.
In the case of a two-ray channel model applied to Tr01, the cumulative sum of the distribution of the measured coherence times is depicted in Figure 4, where 90% of the multipath rays has a life span of almost 70ms. Shorter coherence times are measured on the other reference tracks, proportionally to the simulated train velocity.

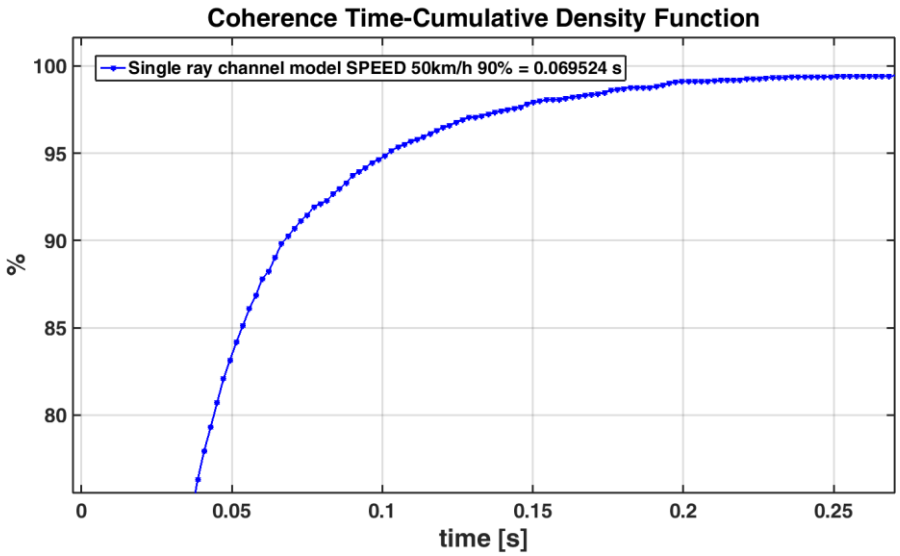

Figure 4. Tr01: Coherence Time for a two-ray channel model.

2.2.2.1.3 *Pseudorange errors*

Another metric to assess the behaviour of the two-ray simplification of the channel model is the ***evaluation of the induced pseudorange error in a reference receiver***. The errors induced on the pseudorange measured by a receiver may depend on the track characteristics and on the elevation of the satellite. For this reason, we report in Table 2 the statistics of such errors for the original multi-ray model compared to the simplified two-ray model.

Table 2 - Tracking error statistics for multi rays and two rays channel models

Track ID	Satellite elevation	Channel model	Tracking errors statistics	
			Mean (m)	Std (m)
Tr01	High	Multi rays	0.22	1.13
		Two rays	0.23	0.69
	Low	Multi rays	0.21	1.20
		Two rays	0.24	0.69
Tr02	High	Multi rays	0.21	1.12
		Two rays	0.22	0.68
	Low	Multi rays	0.26	1.33
		Two rays	0.21	0.70
Tr03	High	Multi rays	0.25	0.96

		Two rays	0.21	0.69
	Low	Multi rays	0.23	1.06
		Two rays	0.21	0.68

We can conclude that the analysed simplification leads to a *decrease in the standard deviation of the tracking error, on the order of 40%-45%* and to *negligible effects on the mean value*.
Furthermore, it is possible to show that the *two-ray model* induces *about 99% of pseudorange errors below 2 m*, whereas with the *multi-ray model* the same error bound is met in *about 91% of the cases*.

2.2.3 Assessment of the radio propagation impact on GNSS measurements

The two-ray HW channel model is intended to be used for configuring an RF signal generator and testing in this way the impact of the simulated radio propagation effects on commercial receivers.
For each reference track in Table 1, the RF signal ensemble is generated twice

1. (Run 0) Without the application of the channel model, to have a reference;
2. (Run 1) Applying the channel model, to observe the propagation channel effects.

The generated signals are elaborated by using a commercial receiver, in the present case a μBlox 6 receiver, which is configured to log both the raw measurements and the PVT results. Then the logs obtained by applying the channel model (Run 1) are compared to the reference ones (Run 0). Figure 5 exemplifies the procedure. The subsections 2.2.3.1 and 2.2.3.2 report the analysis of these results for raw pseudorange measurements and PVT results respectively.

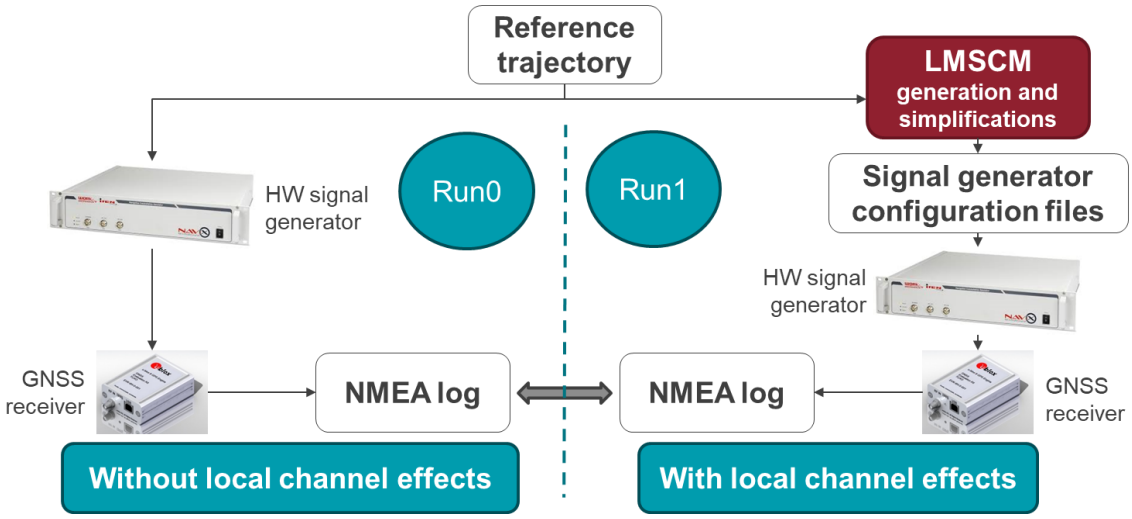

Figure 5. Setup for testing the propagation-induced pseudorange errors.

2.2.3.1 *Raw pseudorange measurements analysis*

The raw measurements considered are the code pseudorange and the phase count. In both cases, the error that affects the Run 1 measurements is statistically analysed in comparison to the corresponding measurements in Run 0, not affected by propagation errors.

The statistical analysis has been repeated for each satellite in view and led to the results reported in the following tables (one table for each track).

PRN	Availability (%)	Code pseudorange errors		Phase count errors	
		mean [m]	std [m]	mean [m]	std [m]
GPS 2	97.8	2.1	4.3	0.05	1.42
GPS 12	99.4	4.7	6.0	-2.49	28.96
GPS 14	99.4	7.0	7.7	-0.06	1.97
GPS 21	100	-1.2	1.5	0.15	0.31
GPS 25	100	-2.2	1.5	0.19	0.33
GPS 26	93.4	12.3	9.7	-0.20	2.82
GPS 29	100	-2.1	1.4	0.11	0.31
GPS 31	100	-1.7	1.7	0.14	0.34
GPS 32	96.1	7.3	8.9	-0.43	2.29

Table 3. Tr01: Raw measurements analysis

PRN	Availability (%)	Code pseudorange errors		Phase count errors	
		mean [m]	std [m]	mean [m]	std [m]
GPS 2	100	0.5	3.7	-0.10	1.29
GPS 12	98.3	1.6	4.6	-0.12	1.08
GPS 14	97.8	2.0	5.0	0.16	1.39
GPS 21	100	-2.6	1.2	0.09	0.27
GPS 25	100	-2.5	1.0	0.1	0.28
GPS 26	93.4	5.0	8.8	0.86	10.86
GPS 29	100	-2.7	1.0	0.01	0.27
GPS 31	100	-2.8	1.0	0.09	0.27
GPS 32	96.1	6.1	7.7	-0.07	1.69

Table 4. Tr02: Raw measurements analysis

PRN	Availability (%)	Code pseudorange errors		Phase count errors	
		mean [m]	std [m]	mean [m]	std [m]
GPS 2	100	-0.7	0.8	0.01	0.18
GPS 12	100	-0.4	0.8	0.04	0.19
GPS 14	100	-0.1	1.0	0.03	0.22
GPS 21	100	-0.9	0.8	0.01	0.17
GPS 25	100	-0.9	0.8	-0.01	0.19
GPS 26	98.9	0.4	2.3	-0.04	0.53
GPS 29	100	-1.0	0.8	0.01	0.19
GPS 31	100	-0.9	0.9	0.01	0.17
GPS 32	99.4	0.3	1.9	-0.01	0.29

Table 5. Tr03: Raw measurements analysis

From the errors reported in Table 3, Table 4, and Table 5 we can see that both the average and the standard deviation of the errors *depend on the position of the satellite in the sky.*

Table 6 reports azimuth and elevation for each satellite and Figure 6 depicts the sky plot; measurements for satellites with high elevation show reduced errors, whereas satellite with low elevation show errors which depends also on the azimuth. Indeed, satellites with low elevation but appearing *along the direction* of the track (N-S) have reduced errors, similar to those at high elevation (e.g., GPS 21).

PRN	Satellite elevation (deg)	Satellite azimuth (deg)
GPS 2	29	51
GPS 12	27	93 *(cross-track)*
GPS 14	22	253 *(cross-track)*
GPS 21	13 *(low)*	184 *(ALONG-TRACK)*
GPS 25	64 *(HIGH)*	78 *(cross-track)*
GPS 26	12 *(low)*	289 *(cross-track)*
GPS 29	87 *(HIGH)*	262 *(cross-track)*
GPS 31	49 *(HIGH)*	299 *(cross-track)*
GPS 32	14 *(low)*	235

Table 6. Tr01, Tr02, Tr03: Elevation and azimuth for each satellite

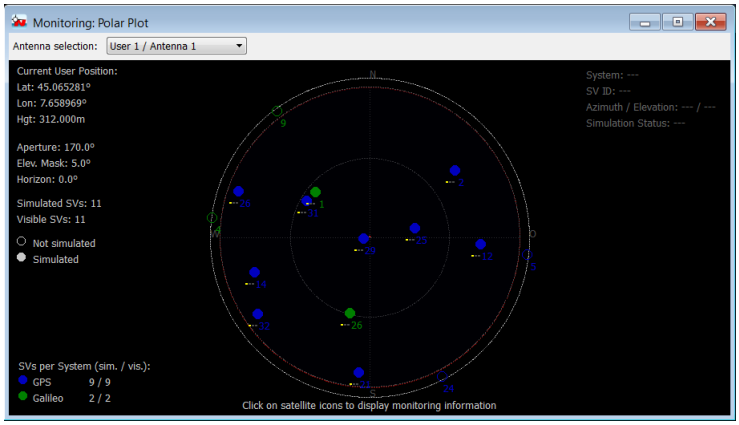

Figure 6. Position of the simulated satellites (screenshot from the signal generator GUI)

Furthermore, different scenarios have different statistics about the presence and the characteristics of the obstacles around the track. The comparison of Table 3, Table 4, and Table 5 show that the *urban scenario* (Tr01) has the largest measurement errors, whereas the *open-sky scenario* (Tr03) exhibits the smallest ones.

As stated before, the probability for each scenario is related to the velocity of the train, where high velocity is typical of an *open sky* environment and low velocity is associated to an urban environment. Moreover, a higher speed of the train implies a shorter duration of the reflected rays and a consequent reduced effect on the tracking stage of the receiver: this is compatible with the lower measurements errors we find in Table 4 and Table 5 for higher velocities.

We can conclude that, with proposed channel model, the measured errors are related to train velocity and the highest measurement errors are related to low velocity.

2.2.3.2 PVT results analysis

The position computed by the GNSS receiver has been compared with the position simulated by the RF signal generator. The statistics of the position error are reported in Table 7 for each track.

Track	Run	Horizontal error, mean (m)	Horizontal error, std (m)	3D error, mean (m)	3D error, std (m)
Tr01	0	0.07	0.04	0.13	0.04
	1	1.40	1.14	1.99	1.14
Tr02	0	0.09	0.04	0.15	0.04
	1	0.80	0.69	2.14	0.69
Tr03	0	0.12	0.03	0.16	0.03
	1	0.24	0.16	0.87	0.16

Table 7. Position error

From Table 7 we can see that the more multipath and fading effects are present, the larger is the positioning error: so, the largest errors are reported for the *urban scenario* (Tr01) which corresponds to the lowest train velocity.
The table reports also results from Run0 for all the tracks as a term of comparison: when the local channel effects are not simulated, then there are no relevant differences amongst the different scenarios.

2.3 Final remarks

The proposed channel model considers the presence of fixed obstacles; some improvements to the model could be added:

- the presence of signal reflections due to the train itself;
- the presence of additional reflected rays to better represent multiple reflections;
- the presence of close moving obstacles (e.g. train moving in parallel rails).

The presence of *reflections from the train top* could be implemented by adding an additional fixed reflected ray to the channel model, analogously to the avionic channel model developed by DLR [14]: however, this addition would decrease the maximum number of satellites supported by the employed hardware simulator. Moreover, this kind of reflections could be attenuated by using a more directional antenna, which excludes all the rays coming from below.

Although the presented two-ray model is able to well represent on average the propagation effects on the pseudorange measurements (see Table 2 and related comments), the higher order statistics are not fully represented (e.g., standard deviation of the pseudorange error). It is expected, however, that the addition of a *second reflection* improves the capability of the HW model to represent the channel statistics. As noted before, the addition of a reflected signal per satellite would proportionally reduce the number of satellite channels that can be generated by the RF simulator.

On the contrary, a specific analysis of the effects of *other trains running on parallel tracks* is not present in literature, so moving obstacles are not included in this channel model. However, the proposed RF channel model should grant the flexibility to add the simulation of such effects (e.g., RF interference, fading of the signal, vibration of the antenna, or additional reflected rays), provided that the capabilities of the hardware signal generator are not overcome.

3 Radio frequency interference classification

Trains encounter many different environments along their long paths, therefore their GNSS receivers are expected to be exposed to various kinds of interference on all the used bands. Man-made radio frequency interference to GNSSs remains as one of the most unpredictable and potentially devastating error sources from the receiver's viewpoint. Indeed, the extremely low power at which a GNSS Signal In Space (SIS) is received at the ground level makes it very vulnerable with respect to interference from other signals, whose sources are ground-based and therefore far closer to the receiver than the GNSS satellites. This problem is well known and much literature has been produced to analyse several aspects of this topic (see [15] and references therein).

In this chapter we present a classification of the possible types of interference affecting the GNSS frequency bands [16], limited at least to the rail domain. A proper classification is fundamental for a correct approach to the problem of interference detection and mitigation, since the techniques adopted in the receiver must be customized on the characteristics of the interfering signal to be monitored (e.g., notch filters for Continuous Wave (CW) interferences or pulse blanking technique for pulsed signals).
The analysis and the classifications proposed in the following are based on a wide survey of the available literature [15] to [40]. However it is worth noticing that *the enumeration of the interference sources cannot be exhaustive*, because of the intrinsic non-deterministic nature of the phenomenon and its variability in dependence on several factors (receiver antenna configuration, vicinity of the interfering source, interfering power, receiver front end central frequency and bandwidth, receiver sensitivity, etc…). In fact, it is common situation in live data collections to detect an interference without any clue about its source or spectral characterization.
Nonetheless, based on the data retrieved from the literature, we propose an identification of interference classes as relevant for the project based on:

- Intentionality (Section 3.1)
- Spectral model (Section 3.2)

For the sake of completeness, the frequency plan allocated for the GPS and Galileo is reported in Table 8 and graphically represented in Figure 7.

System	Band	Bandwidth (MHz)	Center frequency (MHz)
GPS	L5 – 1164-1188 MHz	24	1176.45
	L2 – 1217-1230 MHz	20	1227.60
	L1 – 1563-1587 MHz	24	1575.42
Galileo	E5a – 1164-1191.795 MHz	27	1576.45
	E5b – 1191.795-1217 MHz	25	1207.14
	E6 – 1260-1300 MHz	40	1278.75
	E1 – 1559-1591 MHz	32	1575.42

Table 8 - GPS and Galileo frequency allocation

3.1 Sources of interference

Man-made Radio Frequency Interference (RFI) can be **intentional** or **accidental** [17][18]. Intentional interference is aimed at "blinding" the receiver (jamming) or inducing it in error (spoofing/tampering) and can be generated by means of jammers, nowadays easily available on the market or spoofing equipment, significantly more complicated to install and control. **Intentional interference** can be further classified as 'malicious' and 'uninformed' [17]:

- **Malicious** interference is defined as "RFI intentionally transmitted to prevent the use of GNSS (or make its use hazardous) for as many users as possible". Authors of [17] specify that, in case of such type of

RFI, “it makes sense to provide backup services to support transportation and other critical infrastructures”;

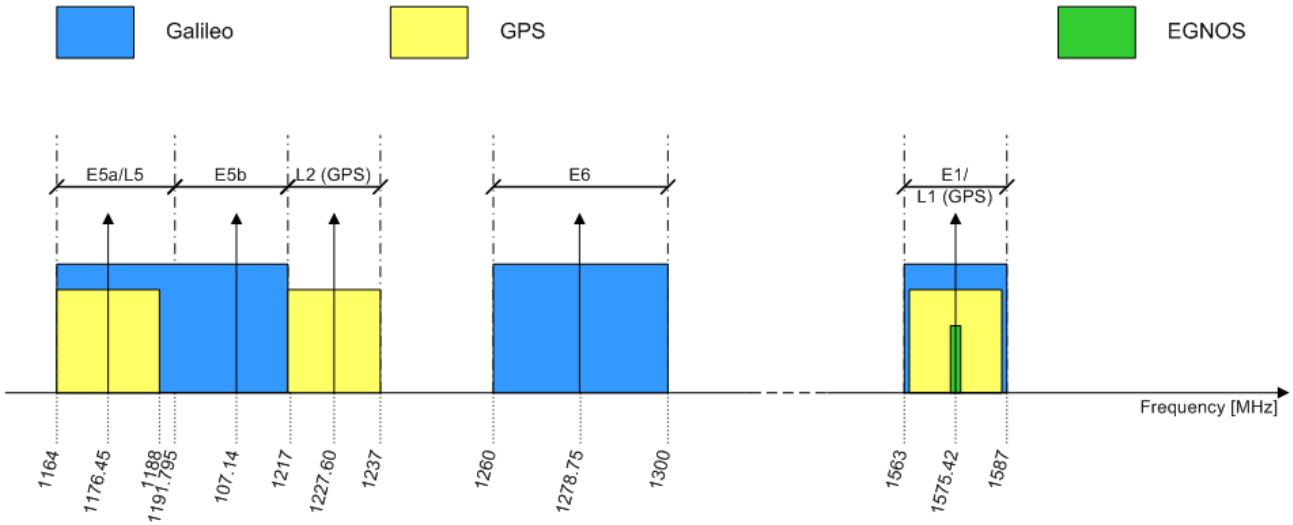

Figure 7: GNSS frequency plan

- **Uninformed** interference on the other hand is the “intentional transmission of interfering signals, but without the desire to cause harm to third parties”. Although this type of interference has always referred to jamming, the spoofing incident detected in the Black Sea over the summer 2017 can be a sort of uninformed spoofing [19][20]. In fact, assuming that the conclusions of [20] are correct (i.e.: the spoofing signals were transmitted for drone defence over a certain area), the effect on GNSS receivers on board of ships can be considered a uninformed effect. Another example of uninformed interference refers to the jamming of GNSS receivers of a Ground Based Augmentation System (GBAS) in an airport, caused by the illegal use of a jammer used by a taxi driver who wanted to hinder his own GPS receiver and block fleet tracking applications [21].

Intentional interference is very challenging to tackle, so that ad-hoc methods to detect and avoid it, often different than those suitable for the unintentional one, have to be adopted.

Accidental (or **unintentional**) interference represents the widest class, because it can be generated by a variety of sources emitting RF signals (often spurious) on the frequency bands where the GNSS receiver operates.

A classification of possible sources of RFI is represented in Figure 8, on the basis of [15] to [40]; they are briefly discussed in subsections 3.1.1 and 3.1.2.

3.1.1 Unintentional RFI sources

Major sources of RFI possibly affecting a GNSS receiver and identified as relevant for the ASTRail project can be the following:

UHF-VHF television and DVB: Second and third harmonics of commercial television broadcasts can occur in the GNSS bands. The digital video broadcasting–terrestrial (DVB-T) is transmitted within the frequency range of 174–230 MHz (UHF band III) and 470–862 MHz (VHF band IV and V) [31]. In addition, several VHF and UHF channels are used in the broadcast analogue TV signals. They can potentially have secondary harmonics close to the L1/E1 carrier, as shown in Figure 9 [31], but the other lower GNSS bands may be interfered too. Spurious emissions of the TV transmitters are required to be attenuated by at least 60 dB. If the transmitter just met the requirement and a third harmonic was broadcast with an EIRP of 0.5 W, a GNSS receiver would be jammed for several kilometers from the interfering source [25]. Interference from analogue

and digital TV transmitters are reported in avionic (en-route flight) [23][25], maritime (coastal and in-harbour operations) [26] and terrestrial applications [28] to [33].

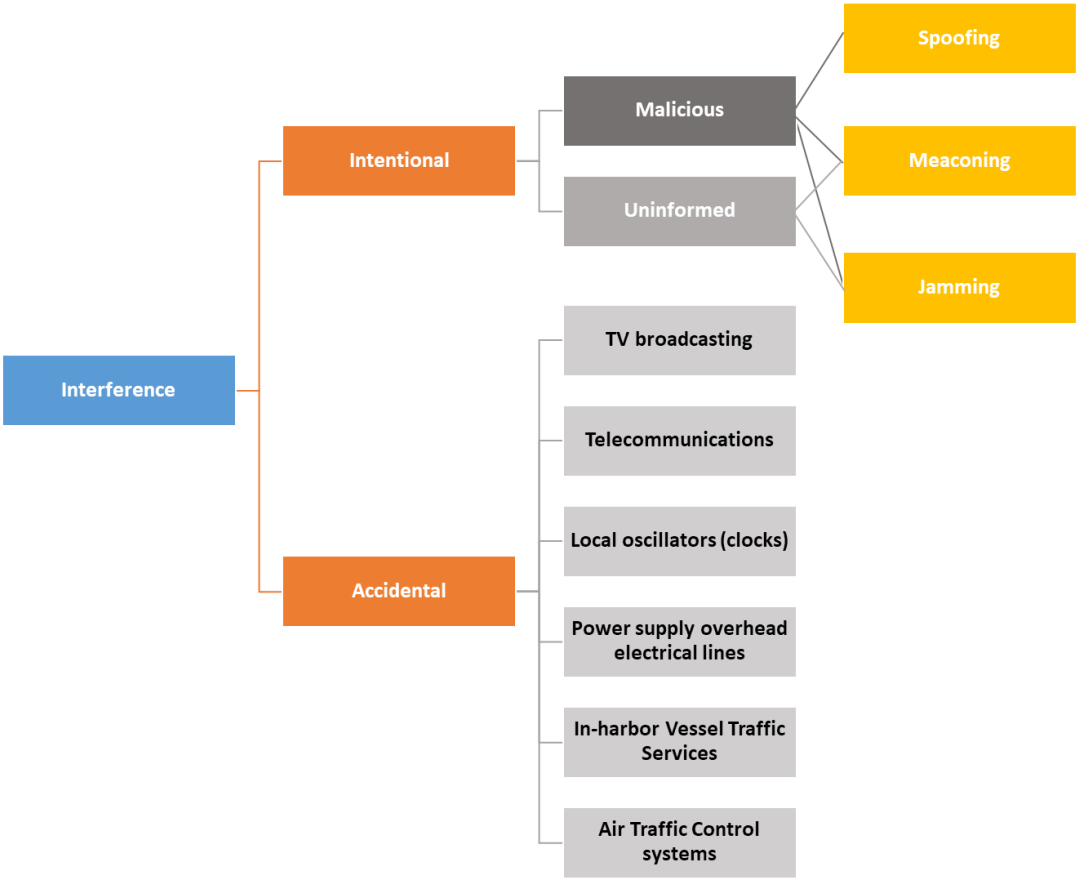

Figure 8: Sources of interference: classification on the basis of their intentionality

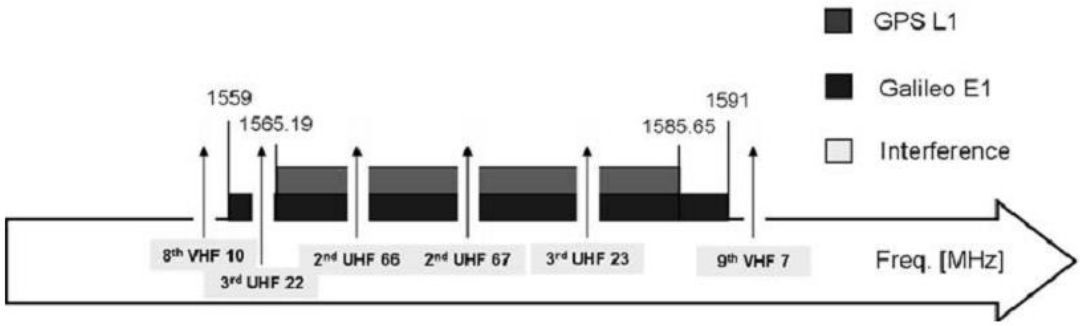

Figure 9: Second and third harmonic interference on the E1/L1 band (from [31])

Telecommunications: Spurious emissions from Power Amplifiers: high power amplifiers working in nonlinearity region are known to generate several spurious harmonics [32], whose effect is sensible on a large band because of the high power at the transmitter.

Surrounding electrical devices: Spurious emissions from oscillators: local oscillators present in most electronic devices (such as personal computers, mobile phones, etc…) can emit spurious harmonics in the GNSS bands [32].

Overhead line equipment in railways: Overhead lines are used to transmit electrical energy to trains at a distance from the energy supply point. They are designed on the principle of one or more overhead wires or rails (particularly in tunnels) situated over rail tracks, raised to a high electrical potential by connection to feeder stations at regular intervals. The feeder stations are usually fed from a high-voltage electrical grid. The high electrical power conveyed along the lines generates spurious magnetic fields that impinge the GNSS antenna as a wideband noise, white in average.

Vessel Traffic Services (VTS): VTS is a marine traffic monitoring system established by harbor or port authorities, similar to air traffic control for aircraft. Typical VTS systems use radars, closed-circuit television, VHF radiotelephony and automatic identification system (AIS) to keep track of vessel movements and provide navigational safety in a limited geographical area. VTS transmissions may generate spurious leakages in the GNSS bands, in forms of harmonics. Although less impacted than those mounted on board of vessels, terrestrial GNSS receivers that operate in the vicinity of the harbor area may sense the interference generated by the VTS transmissions.

Air Traffic Control (ATC) systems: It has been shown that GNSS receivers operating on a civil aircraft are exposed to the signals transmitted from ATC surveillance sensors. If the GNSS receiver is covered within the 3 dB beam-width by the ATC system antenna, the interference is non-negligible [22]. Terrestrial GNSS receivers have low probability of being exposed to ATC transmissions, because such radar systems use directional antennas pointed away from the ground. However, in certain geographical or operational conditions the ATC interference could be sensed also by an Earth-based receiver.
ATC may generate in-band or out-of-band interference on the L5/E5a band, through its Distance Measuring Equipment (DME), and on the E6 band, through the Primary Surveillance Radar (PRS).

3.1.2 Intentional interference

This subsection mentions the most known types of intentional interference (threats) to GNSS signals. All threats foresee the forbidden broadcasting of RF signals over protected bands. Note that a combination of threats is also possible (e.g., jamming first, then spoofing), in order to make the intentional attack more effective. An extensive discussion of such topics is out of the scope of this document; however, an in-depth analysis can be found in [15][35][36] and references therein.

GNSS jamming: Jamming refers to the blocking of the reception of GNSS signals, by deliberately emitting electromagnetic radiation to disrupt user receivers by reducing the signal to noise level [34][35].
The purpose of jamming is to prevent the GNSS receiver from getting the satellite information. This can induce:

- a loss of lock of the GNSS signals tracking (when the jamming power is sufficient enough to saturate the RF stages and/or compromise the digital tracking loops within the receivers); or
- the decrement of the Carrier to Noise power density ratio (C/N_0), which entails a loss of accuracy. This can be considered the worse scenario, because the jamming power is not yet detectable or sufficient to induce the tracking loss of lock, but the positioning accuracy suffers. As correctly recognized in [35], intermediate power values turn out to be the most dangerous cases.

The goal of jamming indeed is not to mislead the receiver's position, but rather to block its operations and totally deny GNSS-based services. Jamming is most often an intentional action (also according to the definition above) but can also occur accidentally, for example due to leakage from strong signals in adjacent bands or noise from other electronic equipment (unintentional interference).
A smarter and more complex format of jamming is represented by the so-called "systematic jamming", recently introduced as a concept in [37]. Systematic jamming attempts to deliberately synchronize short bursts of interference with specific portions of the GNSS signal, where the GNSS is transmitting data indispensable to the receiver for computing the navigation solution. In this way the jammer causes maximum disruption with the minimum power expenditure. As a consequence, detection strategies based on the monitoring of the received signal power, effective against jamming, might fail against systematic jamming.
Since GNSS signals are very weak, deliberate interference can therefore easily defeat the signal recovery or overload the receiver circuitry. This means that jamming a GNSS device is a relatively easy task.

GNSS meaconing: In [38], the meaconing attack is defined as the recording and playback of an entire block of RF spectrum containing an ensemble of GNSS signals. In a meaconing attack, the received signal is not processed during the recording and playback phase. Therefore, the relative time delays and frequency shifts of the signals from different satellites remain the same. The system used to perform a meaconing attack introduces a positive delay, such that the counterfeit signal arrives at the target receiver with a delay relative to the authentic signal.
The effect of a meaconing attack is a decreased position accuracy and, depending on the values of delay and power, a discontinuous estimate of the position (i.e.: the user observes its estimated position "jumping" away). Examples of a meaconing attack can be found in [39], where authors utilize a simple repeater (meaconing) for live testing. Using Commercial Of The Shelf (COTS) components, an effective system can be built with an associated cost of few hundred dollars.
A more complex version of meaconing is discussed in [40]. This attack is still based on the rebroadcast of GNSS signals, but here the attacker intends to finely control the introduced delay and fool in this way any countermeasure based on the monitoring of the clock drift (meaconing with variable delay).
Meaconing attacks are among the most difficult types of intentional interference to detect and mitigate, because they faithfully retransmit the real signals, though impaired by a positive delay. Generally, countermeasures are based on the monitoring of the signal power (to detect abnormal values) and unrealistic time/position jumps.

GNSS spoofing: spoofing attacks are more sophisticated mechanisms, joint by the fact of targeting a specific antenna, whose position need to be known with a certain accuracy; this is also the major difference with respect to the previous forms of intentional interference. A detailed analysis of various forms of spoofing can be found in [35][36].

Malicious interference attacks and the complex techniques to mitigate them are out of the scope of this project, therefore they will be neglected in the following.

3.2 Interference spectral models

Regardless of their source, interfering signals can be classified on the basis of their spectral (and time-domain) characteristics. From a technical viewpoint, this is a fundamental classification, since it distinguishes interfering signals on the basis of their intrinsic characteristics, which allow to identify proper strategies to detect and mitigate their detrimental effects [15][16]. In fact, signals with similar spectral characteristics can be described by similar mathematical models, thus allowing the design of detection/mitigation algorithms tailored to cope with each specific interference model, which encompasses several different sources.
Considering their spectral/temporal characteristics, interfering signals can be grouped in [15][16]:

- **Continuous wave**,
  This class includes all those narrowband signals that can be reasonably represented as *pure sinusoids,* or *a combination* of them*,* with respect to the GNSS band. Many consumer-grade electrical devices, such as personal computer and mobile phones, are equipped with local oscillators that produce harmonics in the GNSS bands [16]. Spurious harmonics can also be produced, in far bands, by high power amplifiers working near saturation, as for instance, those broadcasting analog and digital TV and radio in the UHF/VHF bands, as well as by some radar systems [22].
- **Pulsed**,
  They are characterized by intermittent bursts of signals, such as typically arise from in-band or near-band radars [22][24], or narrowband communication links [29].
- **Swept**,
  They are signals characterized by a narrow instantaneous band at a central frequency that changes over time. These interferences can be *harmonics of FM signals*, produced for instance by TV and radio broadcasting equipment [16]. Swept signal, also known as 'chirp', is also the typical format of the jammers' transmission [34][35].
- **Wideband**,
  Interferences with significant spectral occupancy with respect to the GNSS signals bandwidth can be generically modeled as a wideband noise (white or colored) impacting on the receiver front-end [28]. An example of colored noise sensed in a real terrestrial environment is reported in [29], another might be the interferences produced by the railways power supply equipment. Structured interfering

signals that replicate the GNSS signal format, like in meaconing and spoofing, are other forms of wideband interference.

From this viewpoint, the interference sources identified in Section 3.1 can be classified on the basis of their spectral as shown in Figure 10.

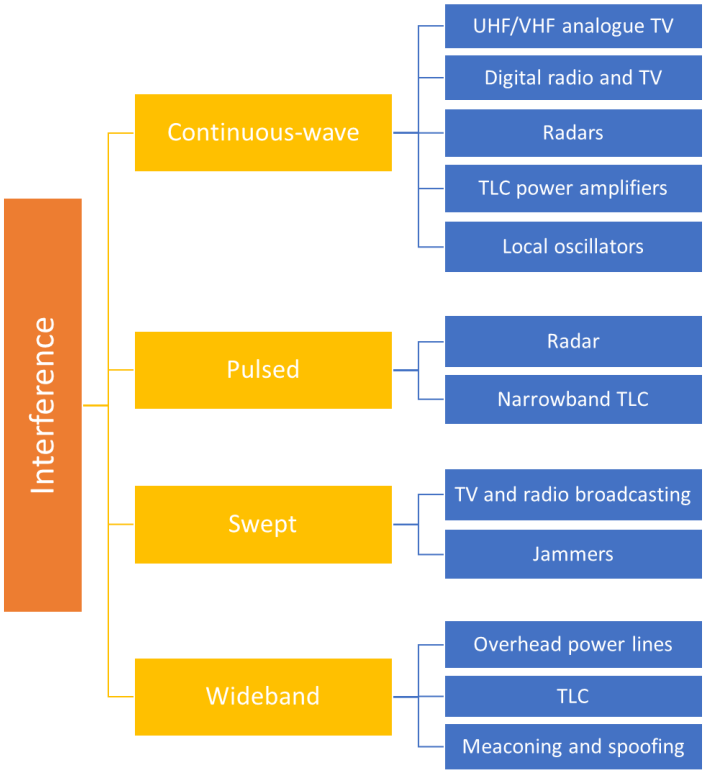

Figure 10: Sources of interference: classification on the basis of their spectral characteristics

3.3 Selection of relevant interference models

As outcome of the previous analysis, we identify the most relevant GNSS interference models for the railways domain, in order to guide the definition and verification of the interference rejection algorithms to be developed in tasks T1.6 – T1.7.

The models we propose to employ are the following:

- Continuous Wave interference;
- Narrowband interference;
- Wideband interference;
- Swept interference;

Their definition parameters are gathered in Table 9, as reference.

Interference signal model	Strength at antenna input level	Interference signal bandwidth	Interference signal centre frequency	Simultaneous events
Continuous Wave	-90 to -75 dBm	0 kHz (spectral line)	In-band: Fixed carrier frequency; anywhere in the nominal receiver bandwidth	Up to two separate spectral lines
Narrowband	-90 to -75 dBm	<= 100 kHz	In-band: Fixed carrier frequency; anywhere in the nominal receiver bandwidth	Up to two separate interfering sources
Wideband	-95 to -75 dBm	(100 kHz, 10 MHz)	In-band: Fixed carrier frequency; anywhere in the nominal receiver bandwidth	One
Swept [41]	-90 to -55 dBm	10 MHz in 20 us (sweep time 20 us)	1575.42 MHz (L1/E1 carrier)	One

Table 9 - Reference interference models

4 Conclusions

This document presented the major impairments that can affect the performance of a GNSS receiver in a railway environment: multipath propagation, NLOS reception, and RFI.
For multipath and NLOS, a channel model present in literature has been selected, adapted to railway environment and analysed. The adaptation led to several advantages with respect to the original channel model:

- Simulation of different scenarios surrounding the train (‘urban’, ‘suburban’, and ‘open-sky’);
- Simulation of complete outages due to the presence of tunnels;
- Support of the RF signal simulation through the use of an RF GNSS signals generator;
- Simulation of an entire GNSS constellation, eased by the employment of the RF GNSS generator;
- Possibility of a direct interface with commercial GNSS receivers to test multipath resilience.

Then, a classification of the main types of RFI is reported along with the selection of the most relevant ones for the railway environment.
It must be noticed that the employment of the RF GNSS signal generator enables to add an RFI to the generated signal in order to test the overall effect on the tested receiver.

List of figures

List of tables

References

[1] N. Kubo, M. Higuchi, T. Takasu, and H. Yamamoto "Performance evaluation of GNSS-based railway applications", 2015 International Association of Institutes of Navigation World Congress, 20-23 October 2015, Prague, Czech Republic.

[2] J. Marais, S. Lefebvre, and M. Berbineau, "Satellite propagation path model along a railway track for GNSS applications", 2004 IEEE 60th Vehicular Technology Conference, Los Angeles, CA, 26-29 September 2004.

[3] J. Marais, M. Berbineau, and M. Heddebaut, "Land mobile GNSS availability and multipath evaluation tool", IEEE Transactions on Vehicular Technology, vol. 54, no. 5, pp. 1697-1704, Sept. 2005.

[4] Lehner, A. Steingass, "A Novel Channel Model for Land Mobile Satellite Navigation," Proceedings of the 18th International Technical Meeting of the Satellite Division of The Institute of Navigation (ION GNSS 2005), Long Beach, CA, September 2005, pp. 2132-2138.

[5] ITU-R P.681-7 (10/09) "Propagation data required for the design of Earth-space land mobile telecommunication systems", October 2009.

[6] E. Falletti, B. Motella, M. Troglia Gamba, C. Facchinetti, "Multipath Mitigation in SoL Environments Using a Combination of Squared Correlators", Proceedings of the 25th International Technical Meeting of The Satellite Division of the Institute of Navigation, ION GNSS 2012, Nashville, TN, September 2012.

[7] P. Brocard, D. Salos, O. Julien, and M. Mabilleau, "Performance evaluation of multipath mitigation techniques for critical urban applications based on a land mobile satellite channel model", 2014 IEEE/ION Position and Navigation Symposium – PLANS 2014, 5-8 May 2014, Monterey, CA (USA)

[8] Report ITU-R P.2145-1: "Model parameters for an urban environment for the physical-statistical wideband LMSS model in Recommendation ITU-R P.681", June 2013.

[9] Fontan, F.P., M. Vazquez-Castro, C. E. Cabado, J. P. Garcia, and E. Kubista, "Statistical modeling of the LMS channel," IEEE Trans. Veh. Technology., vol. 50, pp. 1549–1567, Nov. 2001.

[10] Sciascia, G., S. Scalise, H. Ernst, and R. Mura, "Statistical characterization of the railroad satellite channel at Ku-band," in Proceedings of the International Workshop of Cost Actions 272 and 280, May 2003.

[11] Brocard, P., D. Salos, O. Julien, M. Mabilleau, "Performance Evaluation of Multipath Mitigation Techniques for Critical Urban Applications Based on a Land Mobile Satellite Channel Model", Position, Location and Navigation Symposium - PLANS 2014, 2014 IEEE/ION.

[12] DLR, German Aerospace Agency: http://www.dlr.de/dlr/en/desktopdefault.aspx/tabid-10002/

[13] Power Arches distance: http://www.segnalifs.it/it/ac/N_lineate.htm

[14] A. Steingass, A. Lehner, F. Pérez-Fontán, E. Kubista, M.J. Martín, B. Arbesser-Rastburg, "The High Resolution Aeronautical Multipath Navigation Channel", ION NTM 2004, San Diego, USA, January 26-28, 2004

[15] F. Dovis (Ed.), *GNSS Interference Threats and Countermeasures*, Artech House, 2015. ISBN: 978-1-60807-810-3.

[16] D. Borio and L. Lo Presti "What are the main classes of interferences that can degrade the GNSS signals? What are the possible countermeasures?", Inside GNSS, March-April 2008.

[17] S. Pullen, G.X. Gao, "GNSS Jamming in the Name of Privacy," Inside GNSS, vol. 7, No. 2, Mar./Apr. 2012.

[18] F. Dovis, L. Musumeci, B. Motella, and E. Falletti, "Classification of Interfering Sources and Analysis of the Effects on GNSS Receivers", Chapter 2 in GNSS Interference Threats and Countermeasures, edited by F. Dovis, Artech House, 2015. ISBN: 978-1-60807-810-3

[19] D. Hambling, "Ships fooled in GPS spoofing attack suggested Russian cyberweapon," New Scientist Magazine. Aug. 2017. Online. Available at: https://www.newscientist.com/article/2143499-ships-fooled-in-gps-spoofing-attack-suggest-russian-cyberweapon/

[20] M. Jones, "Spoofing in the Black Sea: What really happened?" GPS World, October 11, 2017. Online. Available at: http://gpsworld.com/spoofing-in-the-black-sea-what-really-happened/

[21] J. C. Grabowsky, "Personal privacy Jammers. Locating Jersey PPDs Jamming GBAS Safety-of-Life Signals", GPS World, Vol. 23, No. 4, April 2012.

[22] M. De Angelis, R. Fantacci, S. Menci, C. Rinaldi, "Analysis of Air Traffic Control Systems Interference Impact On Galileo Aeronautics Receivers" IEEE International Radar Conference, 2005.

[23] A. Italiano, F. Principe, R. Cioni and R. Perago "Multipath and Interference Modelling in Complex GNSS Scenarios", inProc. EuCAP 2010 Conference, Barcellona (Spain), April 12-16, 2010.

[24] G. X. Gao, T. Walter, P. Enge, "DME/TACAN Interference Mitigation in L5/E5 Bands", ION-GNSS 2007.

[25] EUROCONTROL "GNSS frequency protection requirements" EEC Report No. 337, June 1999.

[26] International Association of Marine Aids to Navigation and Lighthouse Authorities "IALA Recommendation R-129 On GNSS Vulnerability and Mitigation Measures" Edition 2, December 2008

[27] J. Marais, "Satellite propagation analysis in a masking environment for GNSS applications", INRETS-LEOST, 2002.

[28] C. Weber, A. Konovaltsev, M. Meurer "Investigation of potentially critical interference environments for GPS/Galileo mass market receivers", 2nd Workshop on GNSS Signals & Signal Processing (GNSS Signal), ESTEC, Nordwijk, Netherlands, Apr. 2007.

[29] T. Jost, C. Weber, C. Schandorf, H. Denks and M. Meurer "Radio Interference Effects on Commercial GNSS Receivers Using Measured Data" ION PLANS 2008.

[30] T. Konefat et al. "Potential EM interference to Radio Services from Railways" Report AY4110 for Radiocomunications Agencies, York EMC Services Ldt, University of York, Heslington, UK, 2002

[31] B. Motella, M. Pini, F. Dovis "Investigation on the effect of strong out-of-band signals on global navigation satellite systems receivers" GPS Solutions, No. 12, pages 77–86, 2008.

[32] R. J. Landry and A. Renard "Analysis of potential interference sources and assessment of present solutions for GPS/GNSS receivers" 4th Int. Conference in Integrated Navigation Systems, 1997.

[33] A. T. Balaei, B. Motella, A. G. Dempster, "GPS Interference Detected in Sydney-Australia" in the Proc. of IGNSS conference, Sydney, December 2007.

[34] H. Ryan *et al.*, "Signal Characteristics of Civil GPS Jammers," GPS World, January 2012. Online. Available at: http://gpsworld.com/gnss-systeminnovation-know-your-enemy-12475/

[35] D. Borio *et al.*, "Impact and Detection of GNSS Jammers on Consumer Grade Satellite Navigation Receivers," Proceedings of the IEEE, vol. 104, No 6, June 2016.

[36] D. Margaria, B. Motella, M. Anghileri, J. J. Floch, I. Fernandez-Hernandez and M. Paonni, "Signal Structure-Based Authentication for Civil GNSSs: Recent Solutions and Perspectives," in IEEE Signal Processing Magazine, vol. 34, no. 5, pp. 27-37. Sept. 2017. doi: 10.1109/MSP.2017.2715898

[37] J. Curran, M. Bavaro, P. Closas, M. Navarro, "On the Threat of Systematic Jamming of GNSS," Proceedings of the 29th International Technical Meeting of the Satellite Division of the Institute of Navigation, ION GNSS+ 2016, Portland, Oregon, pp. 313-321, September 2016

[38] K. Wesson, M. Rothlisberger, T. Humphreys, "A Proposed Navigation Message Authentication Implementation for Civil GPS Anti-Spoofing," Proc. of the 2011 ION GNSS Conference, Portland, OR, Sept. 2011.

[39] D. M. Akos, "GNSS RFI/Spoofing: Detection, Localization, & Mitigation," 2012 PNT Challenges and Opportunities Symposium, Stanford University, November 2012.

[40] K. Wesson, M. Rothlisberger, T. Humphreys, "Practical Cryptographic Civil GPS Signal Authentication," NAVIGATION, Journal of The Institute of Navigation, vol. 59, n. 3, pp. 177-193; Fall 2012.

[41] *Satellite Earth Stations and Systems (SES); GNSS based location systems; Part 3: Performance requirements*. ETSI TS 103 246-3 V1.1.1 (2015-07).